



OPEN ACCESS

EDITED BY

Tao Lin,
New Hope Group, United States

REVIEWED BY

Eduardo Costa,
Wageningen Bioveterinary Research Institute,
Netherlands
Dachrit Nilubol,
Chulalongkorn University, Thailand

*CORRESPONDENCE

Gustavo Machado
✉ gmachad@ncsu.edu

RECEIVED 03 February 2023

ACCEPTED 12 June 2023

PUBLISHED 29 June 2023

CITATION

Sanchez F, Galvis JA, Cardenas NC, Corzo C,
Jones C and Machado G (2023) Spatiotemporal
relative risk distribution of porcine reproductive
and respiratory syndrome virus in the
United States.

Front. Vet. Sci. 10:1158306.

doi: 10.3389/fvets.2023.1158306

COPYRIGHT

© 2023 Sanchez, Galvis, Cardenas, Corzo,
Jones and Machado. This is an open-access
article distributed under the terms of the
[Creative Commons Attribution License \(CC BY\)](https://creativecommons.org/licenses/by/4.0/).
The use, distribution or reproduction in other
forums is permitted, provided the original
author(s) and the copyright owner(s) are
credited and that the original publication in this
journal is cited, in accordance with accepted
academic practice. No use, distribution or
reproduction is permitted which does not
comply with these terms.

Spatiotemporal relative risk distribution of porcine reproductive and respiratory syndrome virus in the United States

Felipe Sanchez^{1,2}, Jason A. Galvis¹, Nicolas C. Cardenas¹,
Cesar Corzo³, Christopher Jones² and Gustavo Machado^{1,2*}

¹Department of Population Health and Pathobiology, College of Veterinary Medicine, North Carolina State University, Raleigh, NC, United States, ²Center for Geospatial Analytics, North Carolina State University, Raleigh, NC, United States, ³Veterinary Population Medicine Department, College of Veterinary Medicine, University of Minnesota, Saint Paul, MN, United States

Porcine reproductive and respiratory syndrome virus (PRRSV) remains widely distributed across the U.S. swine industry. Between-farm movements of animals and transportation vehicles, along with local transmission are the primary routes by which PRRSV is spread. Given the farm-to-farm proximity in high pig production areas, local transmission is an important pathway in the spread of PRRSV; however, there is limited understanding of the role local transmission plays in the dissemination of PRRSV, specifically, the distance at which there is increased risk for transmission from infected to susceptible farms. We used a spatial and spatiotemporal kernel density approach to estimate PRRSV relative risk and utilized a Bayesian spatiotemporal hierarchical model to assess the effects of environmental variables, between-farm movement data and on-farm biosecurity features on PRRSV outbreaks. The maximum spatial distance calculated through the kernel density approach was 15.3 km in 2018, 17.6 km in 2019, and 18 km in 2020. Spatiotemporal analysis revealed greater variability throughout the study period, with significant differences between the different farm types. We found that downstream farms (i.e., finisher and nursery farms) were located in areas of significant-high relative risk of PRRSV. Factors associated with PRRSV outbreaks were farms with higher number of access points to barns, higher numbers of outgoing movements of pigs, and higher number of days where temperatures were between 4°C and 10°C. Results obtained from this study may be used to guide the reinforcement of biosecurity and surveillance strategies to farms and areas within the distance threshold of PRRSV positive farms.

KEYWORDS

PRRS virus, swine disease dynamics, biosecurity, surveillance, local transmission

1. Introduction

Porcine reproductive and respiratory syndrome virus (PRRSV) remains widely distributed across the United States swine industry (1–3). Disease surveillance, vaccination strategies, and biosecurity protocols have played a key role in curbing PRRSV outbreaks; however, variants of the endemic North American (NA-type, type 2) and the European (EU-type, type 1) strain periodically cause outbreaks that lead to significant economic losses (4–9). Outbreaks of PRRSV

in the United States have been shown to exhibit seasonal patterns throughout the country, but vary among swine-producing regions (1, 3, 10–12). In the southeastern United States, PRRSV outbreak patterns are typically characterized by a unimodal peak occurring during the fall and winter months, followed by decreases in incidence during the late spring and summer months (1, 3, 10, 13, 14). Summer outbreaks, while less common, occur sporadically and vary by year (3, 7).

The spread of PRRSV is predominantly governed by direct contacts facilitated by the movement of infected pigs between farms, and indirect contacts also referred to as local transmission or area spread, which encompasses several unmeasured between-farm dynamics occurring at close geographical proximity (1, 15–25). Despite local transmission being the least understood transmission pathway of many infectious diseases in humans and animals (26), several epidemiological processes have been attributed to contributing to the local transmission of PRRSV including, the between-farm movement of contaminated personnel (27, 28), trucks delivering pigs and feed (18, 21), animal by-products delivered via feed (16, 18, 29, 30), equipment (e.g., boots, coveralls, bleeding equipment) (28), and airborne viral particle dispersal (23, 31–35). However, differentiating the contribution of each process remains highly challenging. Moreover, the distance at which each process poses a greater risk to neighboring farms remains poorly understood but is fundamental to the understanding of between-farm transmission dynamics (36). Between-farm transmission mechanisms acting on a local scale may vary in relation to the distance between farms and have been reported to range from 1 km to 35 km (1, 11, 17, 18, 20, 32, 33, 35, 37–39). Some of the local transmission mechanisms are also influenced by local environmental conditions (e.g., temperature, relative humidity, pH), genetic diversity of PRRSV, differences in management and biosecurity levels at different farm types, pig density, and the spatial proximity of susceptible farms to infected farms (farm density) (15, 39–41). Given the high density of farms and pigs in intensive pig production areas across the United States, a better understanding of the distance at which the risk of PRRSV transmission from infected to susceptible farms is increased may support and inform the implementation of targeted biosecurity enhancement and surveillance strategies (42, 43).

In this study, we use an adaptive kernel density approach to derive spatial and spatiotemporal estimates of the variation in PRRSV relative risk. Using the kernel density estimate approach, we (1) define the maximum spatial distance at which farms may spread PRRSV based on the proximity of susceptible farms to infected farms and (2) identify farm types with elevated risk for local transmission of PRRSV. Secondly, we implemented a Bayesian spatiotemporal hierarchical model to account for environmental, on-farm biosecurity features, pig density, farm density, and between-farm contact networks metrics to (3) identify factors associated with the risk of PRRSV local transmission.

2. Materials and methods

2.1. PRRSV data source and processing

PRRSV outbreak data for all production types used in this study were obtained from the Morrison Swine Health Monitoring Project (MSHMP) (2). Outbreak data collection was performed by each production company during outbreak investigations or routine surveillance activities and shared with MSHMP (2). Data obtained

includes information on farm-level outbreaks between November 1st, 2017, through December 31st, 2020, from 2,293 farms belonging to three non-commercially related pig production companies in a dense pig production region of the United States. Information about each farm includes, pig capacity, a unique farm identification number, geographical coordinates (hereafter geolocations), production type, and date of confirmed PRRSV outbreak via PRRSV positive laboratory results. Additionally, the Euclidean distance between farms was calculated using farm geolocations. Production types in our farm population ($n=2,293$) were classified as finisher ($n=1,458$, premises that raise pigs from approximately 10 weeks of age until reaching market weight at approximately 5–6 months of age and include wean-to-finish, and feeder-to-finish), nursery ($n=468$, premises that raise piglets from weaning from approximately 3 weeks of age to about 10 weeks of age), isolation ($n=33$, premises specialized in holding breeding or genetic research animals for a temporary period of time), boar stud ($n=15$), and sow ($n=319$, premises with breeding, gestation and/or farrowing rooms and includes farrow-to-wean and farrow-to-feeder farms).

Farms were divided into cases and controls, where cases were defined as any farm that reported an outbreak during the time period of interest, and controls are farms that did not report an outbreak. PRRSV case and control data were split into years (2018, 2019, and 2020) and a seasonal classification (PRRSV season). We defined the PRRSV season as a six-month period from November 1st through May 31st, which represents a time period where increases in farm-level PRRSV incidence have been previously described for the region of the United States considered in this study (3, 14).

2.2. Spatial PRRSV relative risk

Spatial kernel density-ratio, also known as spatial “relative risk” (hereafter risk), is an exploratory approach used to describe the geographical variation in disease risk based on the distribution of PRRSV outbreaks (cases) and the underlying at-risk (controls) population (44–47). PRRSV risk (x) was estimated for each farm ($x = \{x_1, \dots, x_n, n = 2,293 \text{ farms}\}$) in each year and PRRSV season. Farms can report several PRRSV outbreaks in a given year or PRRSV season; however, for the spatial risk analysis, we defined cases as farms that reported at least one PRRSV outbreak, and controls as the remaining farms that did not report an outbreak for a given year and PRRSV season (46). We identified a total of 245 cases in 2018, 190 cases in 2019, and 165 cases in 2020. For the PRRSV seasons, a total of 227 cases in the 2017–2018 PRRSV season, 167 cases in the 2018–2019 PRRSV season, and 148 cases in the 2019–2020 PRRSV season were used. A nonparametric kernel density-ratio approach was used to estimate the risk $p(x)$ for each farm location (x) in each year and PRRSV season as follows:

$$\hat{p}(x) = \log \hat{f}(x) - \log \hat{g}(x) \quad (1)$$

where $\hat{f}(x)$ represents the log density estimates of cases and $\hat{g}(x)$ represents the log density estimates of controls. The natural log is used to symmetrize the treatment of the density estimate ratios, with $p(x) > 0$, representing areas of medium to high PRRSV risk (high concentrations of cases relative to controls), and $p(x) < 0$, representing areas of low PRRSV risk (low concentration of cases relative to controls) (45–48). Calculating spatial risk relies on the selection of an optimal bandwidth

(the maximum distance at which local transmission is unlikely to occur) which directly drives the decline of the risk probability (kernel) given the geolocation of a farm (45, 46, 87). Given the heterogeneous distribution of farm density in our study area, we used an adaptive smoothing approach that allows the bandwidth of each kernel to vary depending on the density of farms (cases and controls) at a given farm geolocation (49). This method reduces smoothing at locations where the density of farms is high (e.g., 10–20 farms per 5 km²), and increases the amount of smoothing in areas where farm density is low (e.g., 1–5 farms per 5 km²) (49). Adaptive smoothing requires the selection of pilot and global bandwidths, where the pilot bandwidths (i.e., cases and controls have a separate fixed distance), and the global bandwidth (i.e., cases and controls have a shared fixed distance), which is a smoothing parameter that adjusts the pilot bandwidth in areas where case and control densities are similarly distributed (45). Here, we compared two different approaches— asymmetric and symmetric adaptive smoothing—for the selection of the pilot bandwidths (Supplementary material S1; Supplementary Figures S1–S6). Pilot and global bandwidths were then used to calculate $\hat{f}(x)$ and $\hat{g}(x)$. Spatial risk (Equation 1) was then calculated by using $\hat{f}(x)$ and $\hat{g}(x)$, and applying a uniform edge-correction, which accounts for the probability loss of farm geolocations close to the boundary of the study region (45, 46). Lastly, we used 1,000 iterations of Monte Carlo simulations to delineate areas of significant spatial risk ($p < 0.05$) (50). Farms within areas of significant risk were quantified as the count of case or control farms falling within areas of significant spatial risk by farm type.

2.3. Spatiotemporal PRRSV relative risk

The spatiotemporal risk of PRRSV was estimated in weekly time steps of cases for each year and PRRSV season, thus cases were defined as farms with at least one outbreak per week and controls as farms that did not report outbreaks for a given week. The entire farm population ($n = 2,293$) is considered in each weekly time step. A total of 438 cases with an average of 8.76 cases/week were used in 2018, 279 cases with an average of 5.47 cases/week in 2019, and 238 cases with an average of 4.67 cases/week in 2020. Similarly, a total of 382 cases with an average of 12.7 cases/week were used for the 2017–2018 PRRSV season, 231 with an average of 7.45 cases/week in the 2018–2019 PRRSV season, and 190 with an average of 6.33 cases/week in the 2019–2020 PRRSV season. In contrast to the spatial risk, the spatiotemporal risk uses spatial and temporal bandwidths derived from farm geolocations of cases to generate density estimates of cases, while density estimates for controls were generated using only the spatial bandwidth previously calculated for cases since we assume the farm population to be static between November 1st, 2017 and December 31st, 2020 (48, 51, 52). Thus, conditional spatiotemporal risk surfaces were derived as:

$$\hat{p}(x|t) = \log \hat{f}(x,t) - \log \hat{f}(t) - \log \hat{g}(x) \quad (2)$$

where $\hat{p}(x|t)$ is the conditional risk, $\hat{f}(x,t)$ is the log density estimates of cases at a given time step $t = (t_1, \dots, t_w)$, $w = 52$ weeks per year; $w = 30$ weeks per PRRSV season), $\hat{f}(t)$ is an estimator for the marginal temporal case density, and $\hat{g}(x)$ is the static spatial log density of the controls (48). One thousand iterations of Monte Carlo

simulations were used to delineate areas of significant spatiotemporal risk ($p < 0.05$) (50).

Spatiotemporal risk values generated for the entire farm population at each time step (t) were extracted to individual farm geolocations (x). Farms were then classified as low, medium, and high risk based on quantiles of the spatiotemporal risk distribution of all the farms in each year and PRRSV season. Spatiotemporal risk above 60% of the risk distribution was considered as the exceedance risk threshold (53) since it represented a midpoint between lower (negative) and higher (positive) risk values for the years and PRRSV season. Thus, farms with risk below 60% of the risk distribution were categorized as low risk, 61 to 80% quantile as medium risk, and 81 to 100% quantile as high risk for each year and PRRSV season (Supplementary Figures S7–S12).

2.4. Priority index

The priority index (PI) is a metric that has been used to facilitate the communication of spatiotemporal risk (54). The aim of the PI is to provide an easily interpretable metric, represented as an ordered percentage that indicates the level of prioritization that should be given to a farm based on the estimated risk. The priority index was calculated from the spatiotemporal risk weekly estimates as:

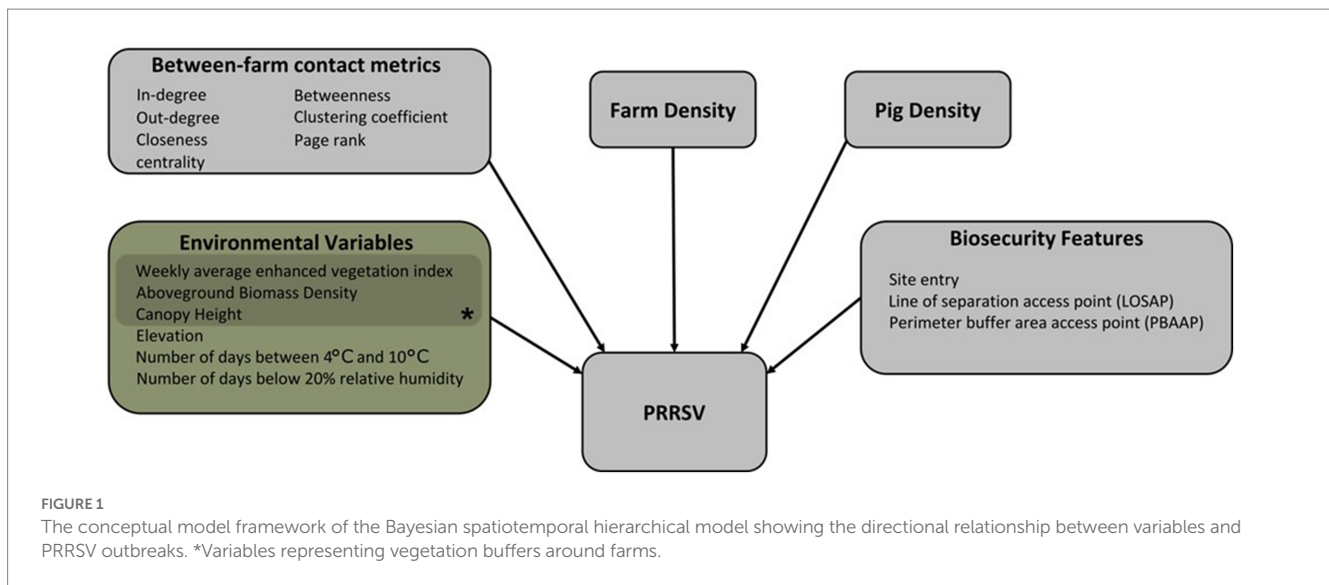
$$PI = \hat{p}(x|t) / \max(\hat{p}(x|t)) * 100 \quad (3)$$

where the PI of a farm is a percentage based on the risk $\hat{p}(x|t)$ of a farm in reference to the maximum risk value of the farm population. Priority indices calculated for each farm were further reclassified as low (0–30%), medium (31–60%), and high (61–100%) priority classifications based on quantiles. Priority index classifications were then summarized by farm types for each year and PRRSV season time periods and used to set the priority risk order of each farm type.

2.5. Bayesian spatiotemporal hierarchical model framework

We fit a Bayesian spatiotemporal hierarchical model of PRRSV weekly outbreak data to account for three on-farm biosecurity features, six between-farm contact network metrics, six environmental variables, farm density, and pig density (Figure 1; Supplementary material Table S1). A total of 1,948 farms out of our 2,293 farms were used in the Bayesian spatiotemporal hierarchical model, since 217 farms lacked between-farm contact data, 124 lacked on-farm biosecurity features, and four lacked environmental data. Additionally, between-farm contact data was not available for the entire study period; therefore, the Bayesian spatiotemporal hierarchical model was implemented for the year 2020. Farm geolocations i ($i = i_1, \dots, i_n$, $n = 1,948$ farms in the year 2020) were defined as $Y_i = 1$ when a PRRSV outbreak was reported, and $Y_i = 0$ for farms with no reported outbreaks of each week in the year 2020. The generalized hierarchical spatiotemporal model was implemented as a logistic regression, where Y_i follows a binomial distribution:

$$Y_i \sim \text{Bernoulli}(\mu_i) \quad (4)$$



and linear predictors were constructed as:

$$\text{Logit}(\mu_i) = \alpha + X\beta + v(i) + \text{week}(w) + \omega(i) \quad (5)$$

where α represents the probability of a PRRSV outbreak, α the model intercept, $X\beta$ describes the matrix of covariates, $v(i)$ is an independent and identically distributed (iid) random effect to account for variation between individual farms, $\text{week}(w)$ is an iid random effect to account for variation between weeks, and $\omega(i)$ represents a spatial random field (Gaussian field) to account for spatial errors (55).

Briefly, the regression analysis was implemented with a stochastic partial differential equation (SPDE) model using integrated nested Laplace approximations (INLA) (56–60). The process first requires the creation of a mesh of Delaunay triangulations, which includes the specification of the maximum triangle edge length, and the model domain boundary. The resulting mesh (Supplementary Figure S13) consisted of 4,504 triangle vertices, where the model domain boundary was defined by a polygon representative of our study area in which the maximum triangle edge length was specified as 10 km within the inner domain and 20 km in the outer domain (55).

The INLA default priors were used; therefore, the penalized complexity (PC) priors [(1, 0.01), (0.32, 0.01)] were used for the spatial random fields where the spatial range and standard deviation quantile and probability tailored to be higher than 1 is 0.01 (59, 61, 62). Model fixed effect outputs were exponentiated and presented as odds ratio (63, 64). The sensitivity of priors to the posterior random field values was examined by comparing the random posterior mean distribution values of PC priors against log-gamma priors [(1, 0.05), (1, 0.001)] (Supplementary Figure S14).

2.6. Bayesian spatiotemporal hierarchical model data preparation

Variables considered in our Bayesian spatiotemporal hierarchical model framework focus on local transmission mechanisms, and

environmental or anthropogenically mediated factors that may contribute to increases or decreases in risk of PRRSV outbreaks (Figure 1; Supplementary material Table S1) (1, 3, 19, 20, 23, 25, 65–67). On-farm biosecurity feature data were extracted for each farm from a database of Secure Pork Supply (SPS) biosecurity plans assembled by the Rapid Access Biosecurity app (RABapp™) (68) and included: the count of site entries, count of perimeter buffer area access points (PBAAP), and count of lines of separation access points (LOSAP) (Supplementary Figure S16; Supplementary material Table S1). In addition to on-farm biosecurity features, we included pig capacity, and farm density, which was calculated by creating a spatial buffer of 17 km around each farm location and counting the number of farms within the buffer. A spatial buffer of 17 km was used based on findings from the spatiotemporal kernel density approach discussed in further detail in section 3.2.

A directed and static network was reconstructed from between-farm pig movement data between January 1st, 2020, and December 31st, 2020, and represented as a graph $g = (V, E)$, where V represents the nodes (farm) of the network and E represents the contact between two nodes or edges of the network. The unique farm identification number in each origin and destination movement record was used to form the edges of the network (69). Between-farm contact network metrics: in-degree, out-degree, PageRank, clustering coefficient, closeness centrality, and betweenness were calculated to characterize node and network-level features of the directed, static network and are described in Supplementary material Table S1. A total of 217 farms were missing pig movement data in 2020, and thus were excluded from this dataset. Therefore, between-farm pig movement data belonging to 1,948 farms was used to calculate between-farm contact network metrics considered in the Bayesian spatiotemporal hierarchical model framework (Figure 1).

Individual farm geolocations were used to extract environmental variables: weekly enhanced vegetation index (EVI), downloaded from the National Aeronautics and Space Administration (NASA), Moderate Resolution Imaging Spectroradiometer (MODIS) Land Products (70), and yearly averages of aboveground biomass density (AGBD), canopy

height, and land surface elevation, downloaded from the Oak Ridge National Laboratory, Distributed Active Archive Center for Biogeochemical Dynamics website (ORNL DAAC) (71). These variables are meant to represent topographical or vegetative buffers around farms that reduce or facilitate the spread of airborne particulate matter and PRRS virus (1, 72–75). Similarly, farm geolocations were used to extract daily average land surface temperature, and relative humidity data from Daymet: Daily Surface Weather Data (76). Temperature and relative humidity have been shown to impact the infectivity and stability of PRRSV (41, 65, 67), and were included in our model as the count of days a farm geolocation i was associated with temperatures between 4°C and 10°C [$T(4^{\circ}\text{C}, 10^{\circ}\text{C})$] [e.g., farm geolocation i had 20 days of $T(4^{\circ}\text{C}, 10^{\circ}\text{C})$ over the studied period], and the count of days a farm geolocation i was associated with relative humidity below 20% ($\text{RH} < 20\%$) (e.g., farm geolocation i was 30 days on $\text{RH} < 20\%$ over the studied period). All variables listed above were downloaded at a 1 km x 1 km spatial resolution and are described in further detail in [Supplementary material Table S1](#). A total of 71 farm geolocations were outside the data availability range of the AGBD, canopy height, or land surface elevation data products; therefore, data from the nearest farm [average = 5 km (min = 446 m; max = 9.8 km)] within a 10 km radius with complete data were used. Four farms were beyond the 10 km threshold and were excluded from the analysis ([Supplementary Figure S15](#)).

2.7. Bayesian spatiotemporal hierarchical model variable selection and model comparison

All variables considered in our model framework ([Figure 1](#)) were first examined via univariate analysis following the model established in Equation 5, and significance was determined by the 95% credible intervals (CI) in which estimates did not cross one, and the model fit was evaluated using the Watanabe-Akaike information criteria (WAIC). Before selecting variables for the multivariate model, multicollinearity between variables was examined by calculating Pearson's correlation coefficient (r), where significant ($p < 0.05$) correlations above 0.6 were considered highly correlated and would limit our ability to determine individual effects on PRRSV outbreaks. The variables $T[4^{\circ}\text{C}, 10^{\circ}\text{C}]$ and $\text{RH} < 20\%$ ($r = 0.98$), biosecurity features LOSAP and PBAAP ($r = 0.79$), and network metrics, page rank and in-degree ($r = 0.69$) were highly correlated. All other variables were below 0.6 or had insignificant correlations. Among highly correlated variables, the variable yielding a lower WAIC in the univariate analysis was selected for the multivariate model variable selection process. A backward elimination process was carried out starting with all significant variables retained from the univariate analysis. Insignificant variables from the multivariable model were removed one-by-one and the best-fitting model was selected based on the WAIC. Given the high density of farms in our study area, farm density was included in the multivariate analysis as a confounding factor.

All data extraction, processing, and analyzes presented in this work were performed in the R (4.2.1) programming language (77) using the packages: tidyverse (78), sf (79), sp (80), spatstat (81), sparr (82), raster (83), igraph (84), MODISstp (70), daymetr (85), INLA (56), inlabru (86), and INLAoutputs (64).

3. Results

3.1. Spatial PRRSV relative risk

The median distance between farms reporting PRRSV outbreaks was 66.7 km (interquartile range (IQR): 39.4 km - 109.3 km) for 2018, 70 km (IQR: 40.4 km - 114 km) for 2019, 61.4 km (IQR: 36.6 km - 98 km) for 2020, and 66 km (IQR: 39 km - 106.4 km) for all years combined. For the PRRSV seasons, the distance between PRRSV cases was 64.6 km (IQR: 38 km - 107.5 km) for the 2017–2018 PRRSV season, 70.7 km (IQR: 40.2 km - 120.5 km) for the 2018–2019 PRRSV season, and 63.4 km (IQR: 37.3 km - 102 km) for the 2019–2020 PRRSV season. The maximum distance the spatial PRRSV risk extended to was, on average, 14.8 km for both the annual and PRRSV seasons. A total of 377 farms in 2018, 91 in 2019, and 321 in 2020 were within high risk areas ($p < 0.05$) ([Table 1](#)). Among the different farm types, sow farms consistently had a higher number of infected farms within areas of significant high risk in both the annual and PRRSV season time periods, while finisher and nursery farms had more control farms ([Table 1](#); [Supplementary material Tables S2–S4](#)). Comparison among years, 2018 ($n = 85$) had the greatest number of PRRSV infected farms within significant high risk areas compared to 2019 ($n = 21$) and 2020 ($n = 57$; [Table 1](#)).

3.2. Spatiotemporal PRRSV relative risk

The spatiotemporal analysis revealed that the maximum distance PRRSV risk extended to was 15.3 km in 2018, 17.6 km in 2019, and 18 km in 2020, and for the PRRSV seasons, 13.6 km in the PRRSV 2017–2018, 19.2 km in the PRRSV 2018–2019, and 18.9 km in the PRRSV 2019–2020. Spatiotemporal risk estimates for the entire farm population in each time step were classified as high, medium, and low risk based on a 60% exceedance threshold where, on average, 20% of the farms were classified as high risk, 20.1% as medium risk, and 59.9% as low risk for all farm types and years combined ([Supplementary Figures S7–S12](#)). Among farm types, boar stud farms were more frequently located in areas of high risk (30% IQR: 27–38%), followed by sow (29% IQR: 27–34%), nursery (19% IQR: 18–22%), finisher (14% IQR: 13–19%) and isolation farms (12% IQR: 9–24%) ([Table 2](#)). However, it is important to note that the higher percentages seen for boar stud farms may be driven by the fewer number of boar stud farms ($n = 15$) in the farm population. Spatiotemporal risk estimates for the PRRSV seasons revealed sow farms were more frequently classified to be in high risk areas (29% IQR: 24–36%) during this time period, followed by boar studs (27% IQR: 20–33%), nursery (21% IQR: 18–24%), isolation farms (12% IQR: 12–30%), and finisher (18% IQR: 16–25%; [Supplementary material Table S5](#)). Among all farm types, finisher farms (63% IQR: 54–74%) and nursery farms (57% IQR: 52–67%) were consistently classified to be in areas of low risk for both the yearly ([Table 2](#)) and PRRSV season time periods ([Supplementary material Table S5](#)).

Our spatiotemporal analysis revealed a seasonal signal, marked by an increase in farms classified as being in high and medium PRRSV risk areas during the fall, winter, and spring months, with varying intensity between farm types, and years 2018 to 2019, and 2019 to 2020 ([Figure 2](#); [Supplementary Figure S8](#)). The signal onset of the seasonal pattern appears to begin at an earlier date [mid-summer (Week 28) to

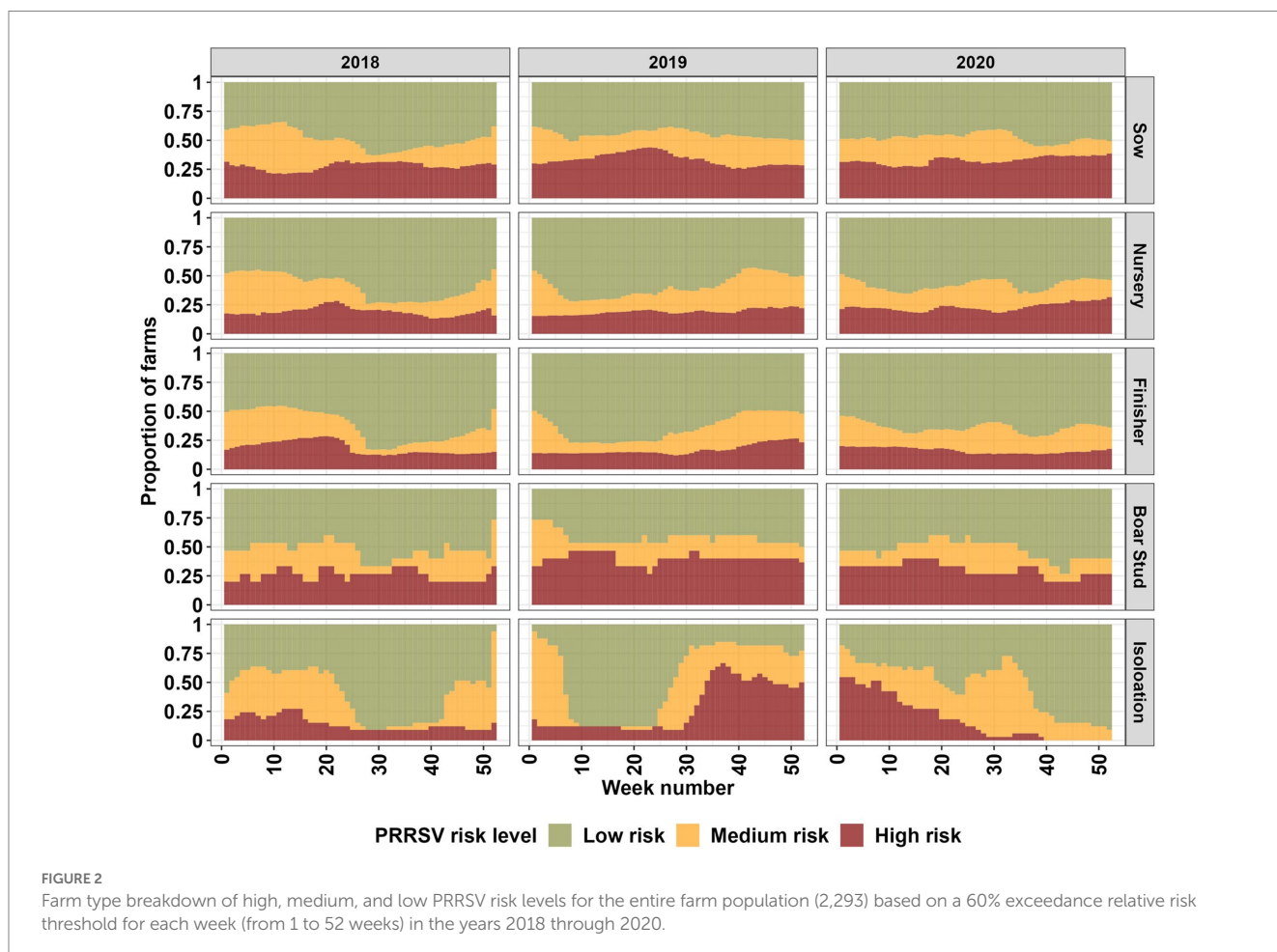
TABLE 1 Yearly count of cases and controls by farm type within significant ($p < 0.05$) high risk areas estimated using a spatial asymmetric adaptive smoothing approach for 2,293 farms (n =number of farms per farm type) in a dense pig production region of the United States.

Year	Sow ($n=319$)		Nursery ($n=468$)		Finisher ($n=1,458$)		Isolation ($n=33$)		Boar Stud ($n=15$)	
	Cases	Controls	Cases	Controls	Cases	Controls	Cases	Controls	Cases	Controls
2018	34	49	13	79	21	126	0	2	0	4
2019	27	21	6	52	5	85	0	1	0	2
2020	44	43	7	81	6	135	0	3	0	3

TABLE 2 Percent of high, medium, and low PRRSV risk levels [median and interquartile range (IQR)] based on weekly risk estimates obtained from the spatiotemporal analysis by farm type for each year and for the entire study period.

Period	Sow			Nursery			Finisher			Isolation			Boar Stud		
	High	Med.	Low	High	Med.	Low	High	Med.	Low	High	Med.	Low	High	Med.	Low
2018	24 (24–29)	22 (17–31)	51 (40–57)	18 (16–21)	21 (15–30)	56 (50–73)	17 (13–25)	20 (10–28)	59 (49–77)	12 (9–19)	39 (19–45)	45 (39–75)	27 (20–27)	27 (20–27)	53 (47–60)
2019	33 (29–37)	16 (14–21)	49 (45–53)	18 (17–20)	16 (11–23)	65 (55–71)	14 (14–20)	17 (6–21)	71 (55–79)	12 (12–48)	21 (12–33)	33 (27–88)	40 (33–40)	13 (7–20)	47 (47–47)
2020	30 (28–35)	27 (16–29)	44 (42–48)	20 (19–25)	22 (20–28)	53 (51–59)	15 (13–16)	25 (21–28)	61 (58–64)	18 (6–29)	42 (24–48)	39 (33–73)	27 (27–33)	20 (13–27)	53 (40–60)
2018–2020*	29 (27–34)	21 (14–28)	48 (43–53)	19 (18–22)	21 (15–26)	57 (52–67)	14 (13–19)	21 (13–26)	63 (54–74)	12 (9–24)	35 (18–45)	42 (33–82)	30 (27–38)	20 (13–27)	47 (47–53)

*Median and IQR for all years combined.



early fall (Week 35)] for the year 2019; however, it is not consistent among all farm types. Sow farms displayed an interesting pattern among farm types, with increases in risk during summer months (Week 20–35) (Figure 2; Supplementary Figure S17). Nursery, finisher, boar stud, and isolation farms appear to show a similar summer

increase in the year 2020, but it is not present for other years. Among all farm types, sow, finisher and nursery farms appear to more closely resemble each other in terms of seasonal risk. Boar stud and isolation show more erratic changes in risk, however, the large shifts in risk levels are related to the small number of farms for these farm types.

Results obtained from calculating the PI, which may be used to order farms in risk priority, revealed that 79.4% of the farms in 2018 were in the low PI category, 16.1% were in the medium PI, and 4.5% were in the high PI category (Supplementary material Table S6). Similarly, 63.7% in 2019 and 67.9% in 2020 were in the low PI category, 28% in 2019 and 23.9% in 2020 were in the medium PI category, and 8.35% in 2019 and 8.28% in 2020 were in the high PI category. Among the different farm types, sow farms consistently had the most farms in the high and medium risk category except boar stud farms in 2019 and 2020; however, as noted before, there are fewer boar stud farms as compared to sow farms in the study population. A similar proportion of farms with high, medium, and low PI overall and by farm type were observed for the PRRSV seasons (Supplementary material Table S7).

3.3. Bayesian spatiotemporal hierarchical model

Results from the univariate analysis revealed that the animal movement network metric, out-degree, the number of LOSAP, number of days the temperature was between T [4°C,10°C], and relative humidity <20% were significantly associated with PRRSV outbreaks (Table 3). The best fitting multivariate model (WAIC=2,620) obtained through backward variable selection included the following variables: out-degree, LOSAP, T [4°C, 10°C], and farm density (Table 3). The strongest association was related to out-going movements, which resulted in an increase in the odds of PRRSV outbreaks by 1.11 times (Table 3). The second most associated variable was LOSAP, with an increase of 1.04 times the odds of PRRSV outbreaks for every additional LOSAP. Lastly, T [4°C, 10°C] resulted in a 1.01 increase in odds for every one unit increase in T [4°C, 10°C].

4. Discussion

We estimated the maximum distance at which the risk of PRRSV is significantly high given the spatial proximity of farms reporting PRRSV outbreaks. Through our spatial and spatiotemporal analysis, we demonstrated that farms within an 11.9km to 17km radius of PRRSV positive farms were at greater risk of being infected due to proximity. PRRSV risk was higher during fall winter and early spring months with variation among the different farm types and years (Figure 2), which is consistent with seasonal patterns previously described for this region of the United States (1, 3, 10, 11, 14). Spatiotemporal risk estimates revealed that approximately 29% of sow farms were consistently located in areas of high risk. We also show that outgoing animal movements (out-degree), the number of barn access points (LOSAP), and the number of days where temperatures were between 4°C and 10°C [T(4°C,10°C)] were risk factors for PRRSV outbreaks (Table 3).

Given the temporal dynamics of PRRSV, and in comparison to the spatial analysis which is a time-static representation of farms reporting PRRSV outbreaks for an entire year and/or PRRSV season, weekly PRRSV outbreak reports were used in our spatiotemporal analysis. Our spatiotemporal analysis showed that the risk of PRRSV transmission from infected farms was significant up to 17km compared to 11.9km in our spatial analysis. We attribute the increase in distance calculated in our spatiotemporal analysis to the density of

TABLE 3 Summary statistics of the fixed effects of the Bayesian spatiotemporal hierarchical models, showing odds ratio (OR), 2.5%–97.5% credible intervals, and WAIC.

Covariate	Univariate			
	OR	CI		WAIC
		2.5%	97.5%	
Pig capacity	1	1	1	2,456.06
Farm density	1	0.99	1	2,462.08
EVI	1.04	0.07	4.65	2,445.97
T[4°C,10°C]	1.02	1.01	1.03	2,421.68
RH < 20%	1.01	1.01	1.02	2,425.71
Aboveground biomass density	1	0.97	1.03	2,449.03
Canopy height	0.96	0.69	1.30	2,459.40
Elevation	1	0.99	1.01	2,457.84
In-degree	1	0.95	1.01	2,456.86
Out-degree	1.11	1.08	1.14	2,397.36
Closeness centrality	-0.14	37.44	229.68	2,448.63
Betweenness	1	1	1	2,454.07
Clustering coefficient	0.28	0.07	1.31	2,451.75
Page rank	0	0	0	2,451.87
Site entry	4.102065 × 10 ⁴	7.698183 × 10 ¹⁴	12.97760 × 10 ¹⁰	13,045.11
PBAAP	1.03	0.98	1.07	2,448.90
LOSAP	1.05	1.02	1.08	2,423.73

Covariate	Multivariate			
	OR	CI		WAIC
		2.5%	97.5%	
Out-degree	1.08	1.11	1.14	
LOSAP	1.01	1.04	1.07	
T[4°C,10°C]	1.01	1.01	1.02	
Farm density	1	1	1.01	
				2,374.83

Bold values correspond to variables that were significant in our analysis.

cases to controls considered in each weekly time step, since we expect that the farm density modulates the size of the bandwidth radius, thus increasing the radius distance to compensate for the low density of cases (46, 87). We remark that the spatial distribution of cases and controls alone may not be sufficient to fully explain PRRSV risk dynamics; therefore, we consider that the maximum distance of 17km calculated in our spatiotemporal analysis reflects a close representation of PRRSV spatial risk in our study region, since risk estimates consider temporal patterns associated with PRRSV (3, 10, 11).

Our spatiotemporal analysis showed increases in PRRSV risk during the fall, winter, and early spring months, which aligns with previous findings for the dense pig production region considered in this study (3, 10, 11, 14). The seasonal effect was consistently detected throughout the study period, but varied in intensity between years and

farm types. In contrast to the typical seasonal patterns previously reported for the dense pig production region considered in this study and continued to be observed in this study, an increase in risk during the summer (Week 20–35) months was detected in sow farms for all years in our study period, with nursery and finisher farms displaying a similar pattern for the years 2018 and 2020, and boar stud and isolation farms only in 2020 (Figure 2). Summer PRRSV outbreaks in breeding and finisher farms have been previously reported (3, 7); however, we show that given the spatial proximity of farms in dense pig production areas, the risk for a PRRSV outbreak may propagate to different farm types. This information supports previous findings and highlights the importance of considering transmission dynamics between farm types during months outside the typical PRRSV season to help farm managers and veterinarians plan for enhanced biosecurity and surveillance (2, 3, 10, 12, 13).

Transmission dynamics of PRRSV involve two main transmission pathways: direct contacts mediated by the movement of infected pigs between farms (18, 20, 25, 66), and indirect contacts referred to as local transmission (1, 11, 15, 16, 18, 19, 23, 33, 66). Local transmission encompasses several mechanisms of spread and is typically used to explain processes that occur over short geographical distances and cannot be attributed to direct contacts caused by live animal shipments among farms (16, 18, 19, 27, 28, 31, 88). Airborne transmission of PRRSV has been suggested as a possible source of local transmission, especially in areas of high farm density; however, evidence has been inconsistent (31). Experimental studies conducted to examine the distance airborne between-farm transmission of PRRSV may occur showed that PRRSV was recovered at a distance of 9.2 km (23, 32). In a recent study, an atmospheric dispersion model was used to determine that farms within a distance of 25 km distance from a PRRSV positive farm were at high PRRSV risk (33). Dispersion models, such as the one developed by (33) may be invaluable tools when conducting outbreak investigations; however, as noted by the authors, further refinement to include environmental factors (e.g., temperature and humidity) and seasonal differences may yield more accurate estimates. In our study, both the spatial (11.9 km - 14.8 km) and spatiotemporal (17 km) distances calculated are within the distances proposed in (23, 33), and given the high density (e.g., 10–20 farms per 5 km²) of farms in our study area, the potential for airborne transmission occurring in our study area cannot be ruled out. However, given the additional mechanisms (e.g., movement of contaminated transportation vehicles, equipment, and personnel) involved in local transmission that have been shown to contribute to the between-farm transmission of PRRSV (18, 28, 89), the small number of samples recovered through airborne transmission (23, 32), and consideration of mechanical (presence of air filtration systems) or environmental factors (e.g., temperature, humidity, vegetation and slope) that may impact the survivability or infectivity of PRRSV, we agree with previous conclusions that airborne transmission is an infrequent or unlikely event (31).

Breeding farms have been the center of most swine disease transmission studies (3, 38, 39, 43, 90–92). In this study, we have shown that the number of sow farms in high-risk areas was larger than all other farm types. A potential explanation as to why sow farms were consistently categorized as high risk may be due to the higher level of systematic testing performed at sow farms as compared to other farm types (2, 18, 19). Higher levels of surveillance in sow farms increase the detection rate of PRRSV outbreaks, consequently increasing the number of analyzed PRRSV outbreaks in our study. Conversely, the

underdetection of downstream farms, which has been noted in previous studies as a limitation to understanding PRRSV transmission dynamics (18, 19, 42, 91, 93), is consistent with our findings in the spatial analysis where large numbers of PRRSV negative farms were within areas of significant high risk. A recent work investigated the association between PRRSV outbreaks and farm proximity to areas of high commingling (slaughterhouses) and found no association; however, the study only considered breeding herds, which highlights the need to consider other farm types that may contribute to disease circulation (43). Our study showed both upstream and downstream farm types within areas of significant risk, and until systematic testing occurs in all farm types, estimations of PRRSV spatial risk will remain a challenge, especially for the estimations for growing pigs. We encourage future research to incorporate parameters that evaluate the sensitivity of the model on the basis of a distribution of possible surveillance levels among the different farm types.

The most important risk factor associated with PRRSV outbreaks in this study was the movement of animals, which has been shown to be the dominant PRRSV transmission route (17, 18, 25, 90, 91, 94, 95–97). Specifically, the effect was related to the out-going movements of animals, which is usually associated with farm types that have large and consistent outgoing shipments of pigs, such as sow and nursery farms. Such farms may usually take on the role of “movement hubs” in a network, thus facilitating the spread of diseases (38, 90, 91, 98). The high number of out-going movements is supported in our findings, where the largest out-degree values were associated with infected nursery farms with a median value of 9 (IQR: 7–11), and 8 (IQR: 6–11) for controls (Supplementary material S2; Supplementary material Table S8). Similarly, positive sow farms had out-degree median values of 6 (IQR: 4–10), and 6 (IQR: 3–10) for controls (Supplementary material Table S8).

The second important variable was LOSAP, which can serve as potential entry pathway for the introduction of pathogens (42, 94). Entry or exit through a LOSAP may involve several risk events such as garbage collection, equipment repair, and removal of cull sows that have been identified as relevant risk events associated with the introduction of diseases (18, 27, 28, 97, 99). Among the different farm types, sow farms had the highest median LOSAP values with control farms having a median value of 5 (IQR: 1–16) LOSAP, and cases having a median value of 3 (IQR: 1–12) LOSAP.

Temperature and relative humidity have been shown to influence the survivability and optimal preservation of infectivity of PRRSV (65, 67). Here, we showed that the increased number of days between 4°C and 10°C and the number of days a farm experienced relative humidity values below 20% increased the probability of PRRSV outbreaks. This is consistent with the seasonal signal of increased risk during the fall and winter months seen in our data and reported in previous research (3, 14). Lastly, we sought to expand on the investigation of the use of vegetation buffers as possible means to mitigate PRRSV transmission. EVI values between 41 and 45, which correspond to dense tree coverage that is consistent with evergreen broadleaf forests were shown to prevent the spread of PRRSV (1). We included EVI, AGB, and canopy height data to capture the structure of the vegetation around the farms; however, these variables were not significant. Given the coarse spatial resolution used in this study, and the benefits of using vegetation buffers to mitigate odor and pathogen emission and introduction (1, 72, 74), we remark that further exploration into the use of remotely sensed data to delineate vegetation buffers is warranted since the availability of imagery from satellites with high temporal and

spatial resolution continues to become more accessible. Lastly, a previous study found the slope of the terrain to be associated with lower PRRSV incidence, with an elevation of 61 meters from sea level determined to be a safe range (1). We did not find a significant correlation between PRRSV outbreaks and land slope in our model; however, we remark that our results may in-part be related to the 1 km x 1 km spatial resolution of our data, and a finer spatial resolution should be explored.

4.1. Limitations and further remarks

The present study has limitations. Firstly, swine production is dynamic in nature, with farms being active and inactive throughout the years. During the time period considered in this study, 34/2,293 farms (1.5%) changed from active to inactive between Nov 1st, 2017 through December 31st 2020, thus we consider our results closely reflect the current status of the swine industry in our study region given the high level of participation of the swine production companies in our study. Another limitation in our study relates to how PRRSV surveillance systems differ between farm types, with sow farms usually conducting routine testing while downstream farm testing is not always performed systematically (39, 42, 93). Differences in systematic testing between the different farm types could have affected our risk estimations; however, we believe that the PRRSV database captured by MSHMP is still the best alternative to the currently available PRRSV datasets (2). For our spatiotemporal analysis, we arbitrarily chose the exceedance risk threshold to be at 60% since it aligned with the interpretation described in (46), where $\hat{p}(x) > 0$ represent areas of higher risk, and $\hat{p}(x) < 0$ areas of low risk. In future studies, other cutoff values should be explored. Additionally, given that a farm may continue to be reported as having an outbreak for multiple weeks, this may potentially influence our spatiotemporal relative risk estimates by increasing the number of cases in a given week. However, since we are interested in quantifying the risk for the potential transmission of PRRSV, it is important we do not omit farms that could contribute to the dissemination of PRRSV. A future study should consider an approach that considers observation autocorrelated in time.

Even though we had to restrict our risk factor analysis to 2020 due to limitations of the between-farm movement data, our results would likely be similar for other years, given how animal movements are vertically integrated in the United States (18, 2, 66, 91, 100). Environmental factors that are known to vary through time were averaged for an entire year, which might dilute the temporal differences in environmental conditions that may influence PRRSV transmission dynamics (3, 13, 14). However, results obtained from this study provide the important groundwork for further exploration of temporal differences related to factors associated with PRRSV local spread. Despite the limitations present in this study, here, we address an important gap related to the spatial range associated with the risk of PRRSV local transmission and estimate the maximum distance to which farms may become exposed and or infected from nearby infected farms. Both results could potentially be used to inform swine producers within areas of elevated risk to consider enhancing surveillance, sampling and disease control strategies (2, 96, 101). In addition, information gathered from this study may be used to calibrate future PRRSV transmission models by considering the

calculated spatial bandwidths as the maximum transmission distance (18–20, 66).

The results of this study suggest that farms within a 17km radius of farms reporting PRRSV outbreaks are at greater risk of infection. We demonstrated that PRRSV outbreaks remain mostly seasonal, with differences in risk intensity between farm types. Our analysis also captured sporadic summer increases in risk, with differences between years and farm types. We found that sow farms had the highest number of cases within areas of significant high risk and were collocated with at-risk finisher and nursery farms. These findings suggest that downstream farms (i.e., finisher farms) may play an important role in maintaining the circulation of PRRSV within the farm population, and support the need for systematic testing among the different farm types. Lastly, out-going movement of pigs, the number of access points and temperature were significant risk factors of PRRSV outbreaks. Ultimately, we provide insights into PRRSV risk dynamics among farm types and establish a maximum distance for the risk of PRRSV local transmission, which could be used to inform targeted surveillance and disease control strategies and calibrate future PRRSV transmission models.

Data availability statement

The datasets presented in this article are not readily available because the data that support the findings of this study are not publicly available and are protected by confidential agreements, therefore, are not available. Requests to access the datasets should be directed to GM, gmachad@ncsu.edu.

Author contributions

FS, CJ, JG, and GM conceived the study. FS, GM, CJ, NC, and JG participated in the design of the study and model formulation. CC coordinated the disease data collection by the Morrison Swine Health Monitoring Program (MSHMP). FS and JG conducted the data processing, cleaning, designed the model, and simulated the scenarios with the assistance of CJ, NC, and GM. FS, JG, NC, GM, and CJ wrote and edited the manuscript. All authors discussed the results and critically reviewed the manuscript.

Funding

This project was funded by the Center for Geospatial Analytics and the College of Veterinary Medicine at North Carolina State University. The Morrison Swine Health Monitoring Project is a Swine Health Information Center (SHIC) funded project. This work was also supported by Food and Agriculture Cyber informatics and Tools, 2020-67021-32462, proposal number 2019-07452 from the USDA National Institute of Food and Agriculture.

Acknowledgments

The authors would like to acknowledge participating companies and veterinarians and the Morrison Swine Health Monitoring Project funded by the Swine Health Information Center.

Conflict of interest

The authors declare that the research was conducted in the absence of any commercial or financial relationships that could be construed as a potential conflict of interest.

Publisher's note

All claims expressed in this article are solely those of the authors and do not necessarily represent those of their affiliated

organizations, or those of the publisher, the editors and the reviewers. Any product that may be evaluated in this article, or claim that may be made by its manufacturer, is not guaranteed or endorsed by the publisher.

Supplementary material

The Supplementary material for this article can be found online at: <https://www.frontiersin.org/articles/10.3389/fvets.2023.1158306/full#supplementary-material>

References

- Jara M, Rasmussen DA, Corzo CA, Machado G. Porcine reproductive and respiratory syndrome virus dissemination across pig production systems in the United States. *Transbound Emerg Dis.* (2021) 68:667–83. doi: 10.1111/tbed.13728
- Perez AM, Linhares DCL, Arruda AG, Van Der Waal K, Machado G, Vilalta C, et al. Individual or common good? Voluntary data sharing to inform disease surveillance systems in food animals. *Front Vet Sci.* (2019) 6:194. doi: 10.3389/fvets.2019.00194
- Sanhueza JM, Stevenson MA, Vilalta C, Kikuti M, Corzo CA. Spatial relative risk and factors associated with porcine reproductive and respiratory syndrome outbreaks in United States breeding herds. *Prev Vet Med.* (2020) 183:105128. doi: 10.1016/j.prevetmed.2020.105128
- Benfield DA, Nelson E, Collins JE, Harris L, Goyal SM, Robison D, et al. Characterization of swine infertility and respiratory syndrome (SIRS) virus (isolate ATCC VR-2332). *J Vet Diagn Invest.* (1992) 4:127–33. doi: 10.1177/104063879200400202
- Holtkamp DJ, Kliebenstein JB, Neumann EJ, Zimmerman JJ, Rotto HF, Yoder TK, et al. Assessment of the economic impact of porcine reproductive and respiratory syndrome virus on United States pork producers. *J Swine Health Prod.* (2013) 21:72–84.
- Jiang Y, Li G, Yu L, Li L, Zhang Y, Zhou Y, et al. Genetic diversity of porcine reproductive and respiratory syndrome virus (PRRSV) from 1996 to 2017 in China. *Front Microbiol.* (2020) 11:618. doi: 10.3389/fmicb.2020.00618
- Kikuti M, Paploski IAD, Pamornchainavakul N, Picasso-Risso C, Schwartz M, Yeske P, et al. Emergence of a new lineage 1C variant of porcine reproductive and respiratory syndrome virus 2 in the United States. *Front Vet Sci.* (2021) 8:752938. doi: 10.3389/fvets.2021.752938
- Valdes-Donoso P, Alvarez J, Jarvis LS, Morrison RB, Perez AM. Production losses from an endemic animal disease: porcine reproductive and respiratory syndrome (PRRS) in selected Midwest US sow farms. *Front Vet Sci.* (2018) 5:102. doi: 10.3389/fvets.2018.00102
- van Geelen AGM, Anderson TK, Lager KM, Das PB, Otis NJ, Montiel NA, et al. Porcine reproductive and respiratory disease virus: evolution and recombination yields distinct ORF5 RFLP 1-7-4 viruses with individual pathogenicity. *Virology.* (2018) 513:168–79. doi: 10.1016/j.virol.2017.10.002
- Alkhamis MA, Arruda AG, Vilalta C, Morrison RB, Perez AM. Surveillance of porcine reproductive and respiratory syndrome virus in the United States using risk mapping and species distribution modeling. *Prev Vet Med.* (2018) 150:135–42. doi: 10.1016/j.prevetmed.2017.11.011
- Arruda AG, Sanhueza J, Corzo C, Vilalta C. Assessment of area spread of porcine reproductive and respiratory syndrome (PRRS) virus in three clusters of swine farms. *Transbound Emerg Dis.* (2018) 65:1282–9. doi: 10.1111/tbed.12875
- Sanhueza JM, Vilalta C, Corzo C, Arruda AG. Factors affecting porcine reproductive and respiratory syndrome virus time-to-stability in breeding herds in the Midwestern United States. *Transbound Emerg Dis.* (2019) 66:823–30. doi: 10.1111/tbed.13091
- Arruda C, Vilalta P, Puig AP, Alba A. Time-series analysis for porcine reproductive and respiratory syndrome in the United States. (Yongchang Cao, Ed.). *PLoS One.* (2018) 13:e0195282. doi: 10.1371/journal.pone.0195282
- Toussignant SJP, Perez AM, Lowe JF, Yeske PE, Morrison RB. Temporal and spatial dynamics of porcine reproductive and respiratory syndrome virus infection in the United States. *Am J Vet Res.* (2015) 76:70–6. doi: 10.2460/ajvr.76.1.70
- Dee J, Deen K, Rossow C, Weise R, Eliason S, Otake HS, et al. Mechanical transmission of porcine reproductive and respiratory syndrome virus throughout a coordinated sequence of events during warm weather. *Can J Vet Res.* (2003) 67:12–9.
- Dee MC, Niederwerder G, Patterson R, Cochrane C, Jones D, Diel E, et al. The risk of viral transmission in feed: what do we know, what do we do? *Transbound Emerg Dis.* (2020) 67:2365–71. doi: 10.1111/tbed.13606
- Galvis JA, Corzo C, Machado G. Modelling porcine reproductive and respiratory syndrome virus dynamics to quantify the contribution of multiple modes of transmission: between-farm animal and vehicle movements, farm-to-farm proximity, feed ingredients, and re-break (preprint). *Ecology.* (2021) 2021:453902. doi: 10.1101/2021.07.26.453902
- Galvis JA, Corzo CA, Machado G. Modelling and assessing additional transmission routes for porcine reproductive and respiratory syndrome virus: vehicle movements and feed ingredients. *Transbound Emerg Dis.* (2022) 69:e1549–60. doi: 10.1111/tbed.14488
- Galvis JA, Jones CM, Prada JM, Corzo CA, Machado G. The between-farm transmission dynamics of porcine epidemic diarrhoea virus: a short-term forecast modelling comparison and the effectiveness of control strategies. *Transbound Emerg Dis.* (2021) 69:396–412. doi: 10.1111/tbed.13997
- Machado G, Galvis JA, Lopes FPN, Voges J, Medeiros AAR, Cárdenas NC. Quantifying the dynamics of pig movements improves targeted disease surveillance and control plans. *Transbound Emerg Dis.* (2020) 68:1663–75. doi: 10.1111/tbed.13841
- Makau DN, Paploski IAD, Corzo CA, VanderWaal K. Dynamic network connectivity influences the spread of a sub-lineage of porcine reproductive and respiratory syndrome virus. *Transbound Emerg Dis.* (2021) 69:524–37. doi: 10.1111/tbed.14016
- Makau DN, Paploski IAD, VanderWaal K. Temporal stability of swine movement networks in the U.S. *Prev Vet Med.* (2021) 191:105369. doi: 10.1016/j.prevetmed.2021.105369
- Otake S, Dee C, Corzo SO, Deen J. Long-distance airborne transport of infectious PRRSV and *Mycoplasma hyopneumoniae* from a swine population infected with multiple viral variants. *Vet Microbiol.* (2010) 145:198–208. doi: 10.1016/j.vetmic.2010.03.028
- VanderWaal K, Perez A, Torremorell M, Morrison RM, Craft M. Role of animal movement and indirect contact among farms in transmission of porcine epidemic diarrhoea virus. *Epidemics.* (2018) 24:67–75. doi: 10.1016/j.epidem.2018.04.001
- VanderWaal K, Paploski IAD, Makau DN, Corzo CA. Contrasting animal movement and spatial connectivity networks in shaping transmission pathways of a genetically diverse virus. *Prev Vet Med.* (2020) 178:104977. doi: 10.1016/j.prevetmed.2020.104977
- Benincà E, Hagenaars T, Boender GJ, van de Kasstele J, van Boven M. Trade-off between local transmission and long-range dispersal drives infectious disease outbreak size in spatially structured populations. (Matthew (Matt) Ferrari, Ed.). *PLoS Comput Biol.* (2020) 16, 16:e1008009. doi: 10.1371/journal.pcbi.1008009
- Galli F, Friker B, Bearth A, Dürr S. Direct and indirect pathways for the spread of African swine fever and other porcine infectious diseases: an application of the mental models approach. *Transbound Emerg Dis.* (2022) 69:e2602–16. doi: 10.1111/tbed.14605
- Pitkin A, Deen J, Dee S. Further assessment of fomites and personnel as vehicles for the mechanical transport and transmission of porcine reproductive and respiratory syndrome virus. *Can J Vet Res.* (2009) 73:298–302.
- Niederwerder M. Risk and mitigation of African swine fever virus in feed. *Animals.* (2021) 11:792. doi: 10.3390/ani11030792
- Ochoa L, Greiner L, Pacion T. Feed as a vehicle for PRRS virus transmission and the effects of formaldehyde on porcine reproductive and respiratory virus in feed: proof of concept. *J Anim Sci.* (2018) 96:63–3. doi: 10.1093/jas/sky073.117
- Arruda S, Toussignant J, Sanhueza C, Vilalta Z, Poljak M, Torremorell CA, et al. Aerosol detection and transmission of porcine reproductive and respiratory syndrome virus (PRRSV): what is the evidence, and what are the knowledge gaps? *Viruses.* (2019) 11:712. doi: 10.3390/v11080712
- Dee S, Otake S, Oliveira S, Deen J. Evidence of long distance airborne transport of porcine reproductive and respiratory syndrome virus and *Mycoplasma hyopneumoniae*. *Vet Res.* (2009) 40:39. doi: 10.1051/vetres/2009022
- Kanankege KST, Graham K, Corzo CA, VanderWaal K, Perez AM, Dürr PA. Adapting an atmospheric dispersion model to assess the risk of windborne transmission of porcine reproductive and respiratory syndrome virus between swine farms. *Viruses.* (2022) 14:1658. doi: 10.3390/v14081658

34. Li P, Koziel JA, Zimmerman JJ, Hoff SJ, Zhang J, Cheng T-Y, et al. Designing and testing a system for Aerosolization and recovery of viable porcine reproductive and respiratory syndrome virus (PRRSV): theoretical and engineering considerations. *Front Bioeng Biotechnol.* (2021) 9:659609. doi: 10.3389/fbioe.2021.659609
35. Otake S, Dee SA, Jacobson L, Pijoan C, Torremorell M. Evaluation of aerosol transmission of porcine reproductive and respiratory syndrome virus under controlled field conditions. *Vet Rec.* (2002) 150:804–8. doi: 10.1136/vr.150.26.804
36. Shea K, Runge MC, Pannell D, Probert WJM, Li S-L, Tildesley M, et al. Harnessing multiple models for outbreak management. *Science.* (2020) 368:577–9. doi: 10.1126/science.abb9934
37. Christianson WT, Joo HS. *Porcine reproductive and respiratory syndrome: A review.* United States: Swine Health Production (1994).
38. Lee K, Polson D, Lowe E, Main R, Holtkamp D, Martínez-López B. Unraveling the contact patterns and network structure of pig shipments in the United States and its association with porcine reproductive and respiratory syndrome virus (PRRSV) outbreaks. *Prev Vet Med.* (2017) 138:113–23. doi: 10.1016/j.prevetmed.2017.02.001
39. Pileri E, Mateu E. Review on the transmission porcine reproductive and respiratory syndrome virus between pigs and farms and impact on vaccination. *Vet Res.* (2016) 47:108. doi: 10.1186/s13567-016-0391-4
40. Dee S, Deen J, Rossow K, Wiese C, Otake S, Joo HS, et al. Mechanical transmission of porcine reproductive and respiratory syndrome virus throughout a coordinated sequence of events during cold weather. *Can J Vet Res.* (2002) 66:232–9.
41. Jacobs AC, Hermann JR, Muñoz-Zanzi C, Prickett JR, Roof MB, Yoon K-J, et al. Stability of porcine reproductive and respiratory syndrome virus at ambient temperatures. *J Vet Diagn Invest.* (2010) 22:257–60. doi: 10.1177/104063871002200216
42. Lambert M-È, Poljak Z, Arsenault J, D'Allaire S. Epidemiological investigations in regard to porcine reproductive and respiratory syndrome (PRRS) in Quebec, Canada. Part 1: biosecurity practices and their geographical distribution in two areas of different swine density. *Prev Vet Med.* (2012) 104:74–83. doi: 10.1016/j.prevetmed.2011.12.004
43. Moeller J, Mount J, Geary E, Campler MR, Corzo CA, Morrison RB, et al. Investigation of the distance to slaughterhouses and weather parameters in the occurrence of porcine reproductive and respiratory syndrome outbreaks in U.S. swine breeding herds. *Can Vet J.* (2022) 63:528–34.
44. Bithell JF. An application of density estimation to geographical epidemiology. *Stat Med.* (1990) 9:691–701. doi: 10.1002/sim.4780090616
45. Davies TM, Hazelton ML. Adaptive kernel estimation of spatial relative risk. *Stat Med.* (2010) 29:2423–37. doi: 10.1002/sim.3995
46. Davies TM, Marshall JC, Hazelton ML. Tutorial on kernel estimation of continuous spatial and spatiotemporal relative risk: spatial and spatiotemporal relative risk. *Stat Med.* (2018) 37:1191–221. doi: 10.1002/sim.7577
47. Kelsall JE, Diggle PJ. Non-parametric estimation of spatial variation in relative risk. *Stat Med.* (1995) 14:2335–42. doi: 10.1002/sim.4780142106
48. Fernando WTP, Hazelton ML. Generalizing the spatial relative risk function. *Spat Spatio Temporal Epidemiol.* (2014) 8:1–10. doi: 10.1016/j.sste.2013.12.002
49. Abramson IS. On bandwidth variation in kernel estimates—a square root law. *Ann Stat.* (1982) 10:1217–23. doi: 10.1214/aos/1176345986
50. Hazelton ML, Davies TM. Inference based on kernel estimates of the relative risk function in geographical epidemiology. *Biom J.* (2009) 51:98–109. doi: 10.1002/bimj.200810495
51. Davies TM, Lawson AB. An evaluation of likelihood-based bandwidth selectors for spatial and spatiotemporal kernel estimates. *J Stat Comput Simul.* (2019) 89:1131–52. doi: 10.1080/00949655.2019.1575066
52. Terrell GR. The maximal smoothing principle in density estimation. *J Am Stat Assoc.* (1990) 85:470–7. doi: 10.1080/01621459.1990.10476223
53. Richardson S, Thomson A, Best N, Elliott P. Interpreting posterior relative risk estimates in disease-mapping studies. *Environ Health Perspect.* (2004) 112:1016–25. doi: 10.1289/ehp.6740
54. Baquero OS, Machado G. Spatiotemporal dynamics and risk factors for human leptospirosis in Brazil. *Sci Rep.* (2018) 8:15170. doi: 10.1038/s41598-018-33381-3
55. Krainski E, Gómez-Rubio V, Bakka H, Lenzi A, Castro-Camilo D, Simpson D, et al. *Advanced spatial modeling with stochastic partial differential equations using R and INLA.* Boca Raton, FL: Chapman and Hall/CRC (2018).
56. Bakka H, Rue H, Fuglstad G, Riebler A, Bolin D, Illian J, et al. Spatial modeling with R-INLA: a review. *WIREs Comput Stat.* (2018) 10:e1443. doi: 10.1002/wics.1443
57. Elias TK, Virgilio GR, Haakon B, Amanda L, Daniela CC, Daniel S, et al. *Advanced spatial modeling with stochastic partial differential equations using R and INLA.* Boca Raton, FL, United States: Chapman & Hall/CRC Press (2019).
58. Lindgren F, Rue H, Lindström J. An explicit link between Gaussian fields and Gaussian Markov random fields: the stochastic partial differential equation approach. *J. R. Stat Soc Ser B Stat Methodol.* (2011) 73:423–98. doi: 10.1111/j.1467-9868.2011.00777.x
59. Rue H, Martino S, Chopin N. Approximate Bayesian inference for latent Gaussian models by using integrated nested Laplace approximations. *J. R. Stat Soc Ser B Stat Methodol.* (2009) 71:319–92. doi: 10.1111/j.1467-9868.2008.00700.x
60. van Niekerk J, Bakka H, Rue H, Schenk O. New Frontiers in Bayesian modeling using the INLA package in R. *J Stat Softw.* (2021) 100:2–10. doi: 10.18637/jss.v100.i02
61. Fuglstad G-A, Simpson D, Lindgren F, Rue H. Constructing priors that penalize the complexity of Gaussian random fields. *J Am Stat Assoc.* (2019) 114:445–52. doi: 10.1080/01621459.2017.1415907
62. Simpson D, Rue H, Riebler A, Martins TG, Sørbye SH. Penalising model component complexity: a principled, practical approach to constructing priors. *Stat Sci.* (2017) 32:576. doi: 10.1214/16-STS576
63. Blangiardo M, Cameletti M. *Spatial and Spatio-temporal Bayesian models with R-INLA.* Chichester, West Sussex: John Wiley and Sons, Inc (2015).
64. Santos Baquero O. *INLAOutputs: Process selected outputs from the “INLA” package.* CRAN (2018).
65. Cutler TD, Wang C, Hoff SJ, Zimmerman JJ. Effect of temperature and relative humidity on ultraviolet (UV254) inactivation of airborne porcine reproductive and reproductive syndrome virus. *Vet Microbiol.* (2012) 159:47–52. doi: 10.1016/j.vetmic.2012.03.044
66. Galvis JA, Corzo CA, Prada JM, Machado G. Modelling the transmission and vaccination strategy for porcine reproductive and respiratory syndrome virus. *Transbound Emerg Dis.* (2021) 69:485–500. doi: 10.1111/tbed.14007
67. Hermann J, Hoff S, Muñoz-Zanzi C, Yoon K-J, Roof M, Burkhardt A, et al. Effect of temperature and relative humidity on the stability of infectious porcine reproductive and respiratory syndrome virus in aerosols. *Vet Res.* (2007) 38:81–93. doi: 10.1051/vetres:2006044
68. Machado G, Galvis JOA, Cardenas NC, Ebling DDS, Freeman A, Hong X, et al. *The rapid access biosecurity (RAB) appTM handbook (preprint).* Open Science Framework (2023).
69. Brandes U, Erlebach T. *Network analysis*, vol. 3418. Berlin, Heidelberg: Springer Berlin Heidelberg (2005).
70. Busetto L, Ranghetti L. MODISp: an R package for automatic preprocessing of MODIS land products time series. *Comput Geosci.* (2016) 97:40–8. doi: 10.1016/j.cageo.2016.08.020
71. ORNL DAAC. *ORNL DAAC for biogeochemical dynamics.* (2022). Available at: <https://daac.ornl.gov/> (Accessed June 11, 2022).
72. Adrizal A, Patterson PH, Hulet RM, Bates RM, Myers CAB, Martin GP, et al. Vegetative buffers for fan emissions from poultry farms: 2. ammonia, dust and foliar nitrogen. *J Environ Sci Health Part B.* (2008) 43:96–103. doi: 10.1080/03601230701735078
73. Arruda C, Vilalta AP, Morrison R. Land altitude, slope, and coverage as risk factors for porcine reproductive and respiratory syndrome (PRRS) outbreaks in the United States. (ram K. Raghavan, Ed.). *PLoS One.* (2017) 12:e0172638. doi: 10.1371/journal.pone.0172638
74. Guo L, Ma S, Zhao D, Zhao B, Xu B, Wu J, et al. Experimental investigation of vegetative environment buffers in reducing particulate matters emitted from ventilated poultry house. *J Air Waste Manag Assoc.* (2019) 69:934–43. doi: 10.1080/10962247.2019.1598518
75. Tyndall J, Colletti J. Mitigating swine odor with strategically designed shelterbelt systems: a review. *Agrofor Syst.* (2006) 69:45–65. doi: 10.1007/s10457-006-9017-6
76. Thornton MM, Shrestha R, Wei Y, Thornton PE, Kao S, Wilson BE. *Daymet: Daily surface weather data on a 1-km grid for North America, Version 4.* (2020).
77. Core Team R. *R: A language and environment for statistical computing.* Vienna, Austria: CRAN (2021).
78. Wickham H, Averick M, Bryan J, Chang W, McGowan L, François R, et al. Welcome to the Tidyverse. *J Open Source Softw.* (2019) 4:1686. doi: 10.21105/joss.01686
79. Pebesma E. Simple features for R: standardized support for spatial vector data. *R J.* (2018) 10:439. doi: 10.32614/RJ-2018-009
80. Bivand R, Pebesma EJ, Gómez-Rubio V. *Applied spatial data analysis with.* 2nd ed. New York: Springer (2013).
81. Baddeley A, Rubak E, Turner R. *Spatial point patterns: Methodology and applications with R.* Boca Raton, London, New York: CRC Press, Taylor and Francis Group (2016).
82. Davies TM, Hazelton ML, Marshall JC. Sparr: analyzing spatial relative risk using fixed and adaptive kernel density estimation in R. *J Stat Softw.* (2011) 39:1–14. doi: 10.18637/jss.v039.i01
83. Hijmans E, Sumner C, Baston D, Bevan A, Bivand R, Busetto L, et al. *Raster: Geographic data analysis and modeling.* (2022).
84. Csárdi G, Nepusz T, Airoldi EM. *Statistical network analysis with Igraph.* New York: Springer (2016).
85. Hufkens K, Basler D, Milliman T, Melaas EK, Richardson AD. An integrated phenology modelling framework in r. (Sarah Goslee, Ed.) *Methods Ecol. Evolution.* (2018) 9:1276–85. doi: 10.1111/2041-210X.12970
86. Bachl FE, Lindgren F, Borchers DL, Illian JB. Inlabru: an R package for Bayesian spatial modelling from ecological survey data. (Robert Freckleton, Ed.) *Methods Ecol. Evol.* (2019) 10:760–6. doi: 10.1111/2041-210X.13168

87. Davies TM, Jones K, Hazelton ML. Symmetric adaptive smoothing regimens for estimation of the spatial relative risk function. *Comput Stat Data Anal.* (2016) 101:12–28. doi: 10.1016/j.csda.2016.02.008
88. Ruston CR. Evaluation of a staged loadout procedure for market swine to prevent transfer of pathogen contaminated particles from livestock trailers to the barn. *J Swine Health Prod.* (2021) 29:234–43.
89. Thakur KK, Revie CW, Hurnik D, Poljak Z, Sanchez J. Analysis of swine movement in four Canadian regions: network structure and implications for disease spread. *Transbound Emerg Dis.* (2016) 63:e14–26. doi: 10.1111/tbed.12225
90. Kinsley AC, Perez AM, Craft ME, Vanderwaal KL. Characterization of swine movements in the United States and implications for disease control. *Prev Vet Med.* (2019) 164:1–9. doi: 10.1016/j.prevetmed.2019.01.001
91. Passafaro TL, Fernandes AFA, Valente BD, Williams NH, Rosa GJM. Network analysis of swine movements in a multi-site pig production system in Iowa, USA. *Prev Vet Med.* (2020) 174:104856. doi: 10.1016/j.prevetmed.2019.104856
92. Paploski IAD, Corzo C, Rovira A, Murtaugh MP, Sanhueza JM, Vilalta C, et al. Temporal dynamics of co-circulating lineages of porcine reproductive and respiratory syndrome virus. *Front Microbiol.* (2019) 10:2486. doi: 10.3389/fmicb.2019.02486
93. Velasova M, Alarcon P, Williamson S, Wieland B. Risk factors for porcine reproductive and respiratory syndrome virus infection and resulting challenges for effective disease surveillance. *BMC Vet Res.* (2012) 8:184. doi: 10.1186/1746-6148-8-184
94. Black NJ, Cheng T-Y, Arruda AG. Characterizing the connection between swine production sites by personnel movements using a mobile application-based geofencing platform. *Prev Vet Med.* (2022) 208:105753. doi: 10.1016/j.prevetmed.2022.105753
95. Haredasht D, Polson R, Main K, Lee DH, Martínez-López B. Modeling the spatio-temporal dynamics of porcine reproductive & respiratory syndrome cases at farm level using geographical distance and pig trade network matrices. *BMC Vet Res.* (2017) 13:163. doi: 10.1186/s12917-017-1076-6
96. Perez AM, Davies PR, Goodell CK, Holtkamp DJ, Mondaca-Fernández E, Poljak Z, et al. Lessons learned and knowledge gaps about the epidemiology and control of porcine reproductive and respiratory syndrome virus in North America. *J Am Vet Med Assoc.* (2015) 246:1304–17. doi: 10.2460/javma.246.12.1304
97. Silva GS, Machado G, Baker KL, Holtkamp DJ, Linhares DCL. Machine-learning algorithms to identify key biosecurity practices and factors associated with breeding herds reporting PRRS outbreak. *Prev Vet Med.* (2019) 171:104749. doi: 10.1016/j.prevetmed.2019.104749
98. Dorjee S, Revie CW, Poljak Z, McNab WB, Sanchez J. Network analysis of swine shipments in Ontario, Canada, to support disease spread modelling and risk-based disease management. *Prev Vet Med.* (2013) 112:118–27. doi: 10.1016/j.prevetmed.2013.06.008
99. Silva GS, Corbellini LG, Linhares DLC, Baker KL, Holtkamp DJ. Development and validation of a scoring system to assess the relative vulnerability of swine breeding herds to the introduction of PRRS virus. *Prev Vet Med.* (2018) 160:116–22. doi: 10.1016/j.prevetmed.2018.10.004
100. Sellman S, Beck-Johnson LM, Hallman C, Miller RS, Owers Bonner KA, Portacci K, et al. Modeling nation-wide U.S. swine movement networks at the resolution of the individual premises. *Epidemics.* (2022) 41:100636. doi: 10.1016/j.epidem.2022.100636
101. Alarcón LV, Allepuz A, Mateu E. Biosecurity in pig farms: a review. *Porc Health Manag.* (2021) 7:5. doi: 10.1186/s40813-020-00181-z